学位論文（博士）

Application of Finite Element Method simulation to stress and strain distributions in scored tablet

2024 年 3 月

星薬科大学大学院　薬学研究科

岡田 信人

Contents

List of publications

1. Mechanical Stress Simulation of Scored Tablets Based on the Finite Element Method and Experimental Verification. Nobuto Okada, Yoshihiro Hayashi, Yoshinori Onuki, Takahiro Miura, Yasuko Obata and Kozo Takayama. Chem. Pharm. Bull., 64; 1142-1148 (2016) <presented in Chapter 1 of this dissertation>

2. Strength Simulation of Scored Tablets Based on the Finite Element Method Using an Extreme Vertices Design. Yoshihiro Hayashi, Nobuto Okada, Kozo Takayama, Yasuko Obata and Yoshinori Onuki. Chem. Pharm. Bull., 66; 727-731 (2018) <presented in Chapter 2 of this dissertation>

Abbreviations

API; active pharmaceutical ingredient
CAE; computer-aided engineering
CS; cornstarch
E; young's modulus
FEM; finite element method
F_D; difference factor
F_o; observed F value
ICH; International Conference on Harmonisation
LAC; lactose
L-HPC; low-substituted hydroxypropyl cellulose
MCC; microcrystalline cellulose
Mg-St; magnesium stearate
MS; mean square
PVP; polyvinylpyrrolidone
QbD; quality by design
RSM; response surface method
RSM-S; response surface method incorporating thin-plate spline interpolation
r; correlation coefficient
ν; poisson rate

General introduction

Drug products do not consist solely of active pharmaceutical ingredient (API). It is only when the API is combined with excipients that are compatible and have the appropriate function, and with the appropriate manufacturing processes and controls, that it becomes a dosage form that can be administered to the patient. There are two forms of administration of drug products, oral and parenteral administration. In particular, oral administration is the most widely used and has many advantages, including simplicity of administration, no significant burden on the patient and applicability to API with various physical properties. [1,2] Therefore, approximately 80% of drug products currently on the market and more than the majority of drug products approved in Japan, the USA and Europe in recent years are oral solid formulations such as tablets and capsules.[3] Tablets are manufactured through several processes, including the API milling process to reduce variation in API particle size and adjust particle size, the granulation process to improve the fluidity of the particles for improved handling and compressibility,[4-7] the mixing process to homogenise the API and excipients, the compression process to compress the powder into tablets[8,9] and the film coating process to coat the tablets to ensure identification and API stability.[10] Many factors such as API properties, types of excipient types and amounts, dosage forms, manufacturing methods and conditions can affect formulation quality, and it is important in formulation development to understand the impact on formulation quality while designing drug products.

In recent years, the "quality by design (QbD)" concept was proposed in the International Conference on Harmonization (ICH) Q8 guidance.[11-13] This guidance recommends establishing a science-based rationale, and the drug product formulation development process should ensure the predefined quality by understanding how these factors have affected the quality of the drug product. But in reality, the developed compounds in the research & development phase are very expensive, and the amount of API that can be used for formulation studies is limited, so it is difficult to fully verify the potential factors that affect drug product quality.

Over the past few years, many simulation methods have been developed to understand the important factors affecting drug product quality, such as modeling the mechanical behavior of pharmaceutical powders during compaction process[14,15] and drug dissolution,[16,17] and fluidized bed granulation processes.[18-20] For example, a research case study has been reported in which simulation was applied to the tableting process to estimate the stress distribution and density distribution inside tablets and to investigate the cause of tableting failure.[21,22] There are also reports of studies on the simulation of swelling and drug release characteristics of hydrophilic polymer-type sustained drug release tablets with different tablet shapes and drug ratios in tablets.[23-25] However, the model formulation and shape which lack practicality are used, and there is a large deviation from the actual formulation.[21,26] Although these studies contain important findings that contribute to formulation quality assurance, they are not directly applicable to actual formulation development.

Podczeck et al. performed FEM simulations of the breaking strength of scored tablet, assuming elastic and elastoplastic models for the tablet components.[27] Although there was little difference between the elastic and elastoplastic models for breaking strength, the direction of the scored line had a significant effect, indicating that the strength could be significantly reduced when the direction of the scored line was more than 45° to the compression axis. The results of Podczeck et al. are questionable, as the area of the fracture surface is smaller when the angle of the split line with respect to the compression axis is 0°.

Therefore, the purpose of this study is to establish that the finite element method (FEM), a form of computer-aided engineering (CAE) simulation, is a useful tool for understanding important factors in formulation development. Tablets are sometimes split in two to adjust the dosage, depending on the API volume and individual patient variability. Therefore, scored tablets that allow tablets to be easily split are desired. Although there are some tablets that are scored line for identification purposes and cannot be split for use, scored line are generally applied with the intention of dividing the tablet.[28-30] However, the relationship between the shape of score and ease of division, uniformity, breaking strength and formulation remains

unclear. In this study to overcome those problems, the effects of the scored shape on the dividing strength and breaking strength of scored tablets were investigated in detail using FEM. Furthermore, the validity of the FEM simulation was experimentally verified by preparing model tablets and measuring their dividing strength and breaking strength.

In chapter 1, the aim of this study was to clarify the effect of score shapes on the essential characteristics of tablets by using FEM simulation. I only focused on the depth and angle of scores in this study as the starting point for the potential use of FEM simulation for the design of scored tablets. In chapter 2, the purpose of this study was to explore differences in stress distribution between these design variables using FEM. I also aimed to determine any relationships between FEM results and tablet hardness using response surface method incorporating thin-plate spline interpolation (RSM-S).

Chapter 1

Mechanical Stress Simulation of Scored Tablets Based on the Finite Element Method and Experimental Verification

1. Introduction

Tablets are the most common solid dosage forms compared to other forms such as powders, granules, and capsules. For the individual treatment of patients, tablets are often divided, and thus, well-designed scored tablets are required for clinical use. van Santen et al.[31] reviewed the advantages, limitations, and performance indicators of the score line on tablets; they reported that for many patients, scored tablets are broken unequally and with difficulty, reducing the compliance and reliance on drug therapy. However, Rodenhuis et al.[32] surveyed the use of scored tablets as a dosage form and found that scored tablets play an important role in patient treatment. Even when lower-dose tablets are available, patients continue to subdivide tablets for ease of swallowing and adapting the dose. The score shapes may have a large influence on the essential characteristics of tablets, such as the dividing strength, halving equality, and breaking strength. Score shapes are typically determined empirically, but they have not always been reasonably designed. Sovány et al.[33] reported that the halving property of scored tablets is affected by tableting machines. Podeczeck et al.[27] simulated the influence of the breaking line position of scored tablets on tensile failure by using a FEM. They demonstrated that the position of the breaking line significantly affected the breaking strength of scored tablets. Although numerous FEM simulation studies evaluating the powder compaction and mechanical strength of tablets have been reported,[34-45] very little is known regarding the mechanical adequacy of score shapes involving dividing strength, halving equality, and breaking strength. The aim of this study was to clarify the effect of score shapes on the essential characteristics of tablets by using FEM simulation. A runnel of triangle pole on the top surface of flat tablets was fabricated as the score shape. The depth and angle of scores were changed as design variables. Other factors such as the tablet shape, thickness, and density may affect the dividing strength, halving equality, and breaking strength. However, I only focused on the depth and angle of scores in this study as the starting point for the potential use of FEM simulation for the design of scored tablets. Stress distributions on the tablet surfaces were simulated after applying an external force. The bending force and diametrical compression were applied to the various types of scored tablets. The adequacy of FEM simulation was evaluated using scored tablets composed

5

of lactose (LAC) and cornstarch (CS) as diluents, microcrystalline cellulose (MCC) as a binder, and low-substituted hydroxypropyl cellulose (L-HPC) as a disintegrant.

2. Materials and methods

2.1. Materials

Lactose (LAC; Tablettose 80) was purchased from Meggle Japan Co., Ltd. (Tokyo, Japan). Cornstarch (CS; Graflow M) was purchased from Nippon Starch Chemical Co., Ltd. (Osaka, Japan). Microcrystalline cellulose (MCC; Ceolus PH-101) was purchased from Asahi Kasei Chemicals Co., Ltd. (Tokyo, Japan). Low-substituted hydroxypropyl cellulose (L-HPC; LH-21) was a gift from Shin-etsu Chemical Co., Ltd. (Tokyo, Japan). Magnesium stearate (Mg-St) was purchased from Wako Pure Chemical Industries, Ltd. (Osaka, Japan).

2.2. Preparation of Scored Tablets

Figure 1 shows a schematic representation of the model scored tablets. Twelve types of scores were fabricated on flat-faced tablets by changing the depth (h=0.50, 0.75, 1.00, 1.50 mm) and angle (θ=45, 60, 75°). All ingredients listed in Table 1 were dried at 75°C for 24 h and sieved through a 60-mesh screen. The sieved ingredients were weighed and mixed in a polyethylene bag for 2 min, except Mg-St, which was used as a lubricant. Finally, Mg-St was added into the powder mixture and blended for 1 min. Next, 200 mg of the mixed powder was compressed at 4 kN into flatfaced scored tablets, 8 mm in diameter, using a hydraulic press (Model PCH-20, NPa System Co., Ltd., Saitama, Japan).
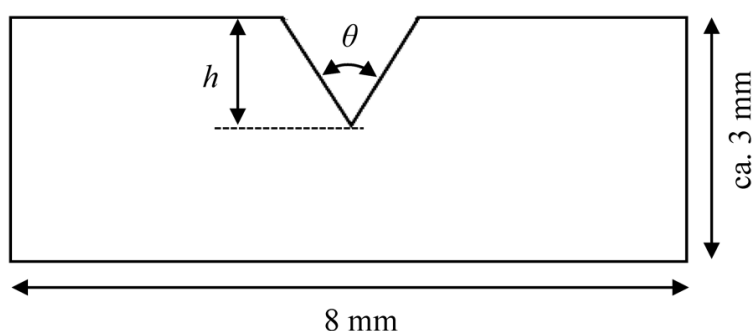

Fig. 1. Geometry of Scored Tablets
Tablets were composed of the powder mixture listed in Table 1. The tablet diameter was 8 mm and the total height was approximately 3 mm. The score depths were 0.50, 0.75, 1.00, and 1.50 mm. The score angles were 40, 60, and 75°.

Table 1. Formulation of Model Scored Tablet

Excipient	Quantity/tablet (mg)	Ratio (%)
Lactose (LAC)	40.8	20.40
Corn starch (CS)	33.5	16.75
Microcrystalline cellulose (MCC)	118.4	59.20
Low-substituted hydroxypropyl cellulose (L-HPC)	6.3	3.15
Magnesium stearate (Mg-St)	1.0	0.50
Total	200.0	100.00

2.3. Determination of Elastic Parameters

Young's modulus(E) and Poisson rate (v) were measured as elastic parameters of the tablets. The methods have been fully described in previous reports.[21,46,47] Briefly, these parameters were estimated using an instrumented hydraulic press (TK-TB20KN; Tokushu Keisoku Co., Ltd., Yokohama, Japan). The axial upper/lower punch forces and displacements, as well as the radial die-wall pressure, were measured during compaction. Compression and decompression speeds were set at 1 mm/s 350 mg of sample powder was used. The relative packing density at 2 MPa was measured according to the volume of the gap between the upper and lower punches to calculate the initial density of the powder bed. E and v values were determined according to the following equations:

$$E = \frac{9GK}{3K + G} \tag{1}$$

$$v = \frac{3K - 2G}{2(3K + G)} \tag{2}$$

where K is the bulk modulus and G is the shear modulus. K and G values were estimated from a stress–strain curve obtained during compression and decompression testing.

2.4. FEM Simulation

In the initial stage of loading the external force onto the tablet, I hypothesized that the tablet represented a continuum elastic model. FEM was applied to estimate the principal stresses generated at the top and lateral surfaces, and along scored lines. To avoid generating a singular point, the shape of the score tip was set to be a fillet surface. The stress distribution was

8

simulated after application of external forces such as bending stress and diametrical compression. The application methods of these external stresses to the scored tablet are illustrated in Figs. 2 and 3. In order to mimic tablet division by hand during the bending simulation, part of the unscored bottom surface of the tablets was fixed at the rigid center line of 0.2 mm wide and 8 mm long (shown as dark gray line), and both ends of the top surface (shown as a dark gray area) were pressurized in the vertical direction at 100 N (Fig. 2). For diametrical compression, the scored tablet was compressed onto a rigid wall by moving the other side horizontally at 100 N (Fig. 3). Stress distributions on the top surface and lateral side contacting the moving wall were estimated by FEM simulation.
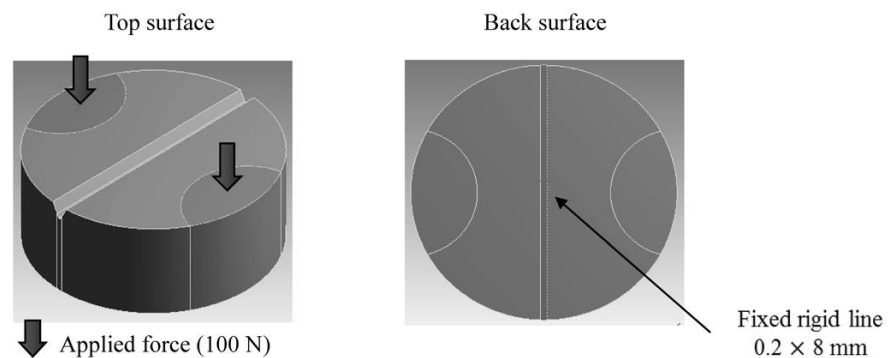
Fig. 2. Method for Applying Bending Force to Scored Tablets
The unscored side of the tablet was fixed by a rigid line that was 0.2 mm wide and 8 mm long. A stress of 100 N was applied to both ends (shown as dark gray area) in the vertical direction.

Fig. 3. Method for Applying Diametrical Compression to Scored Tablets
The right rigid wall was fixed and faced to the lateral side of tablet. The tablet was compressed by moving the left rigid wall horizontally at 100 N.

9

2.5. Determination of Tablet Characteristics

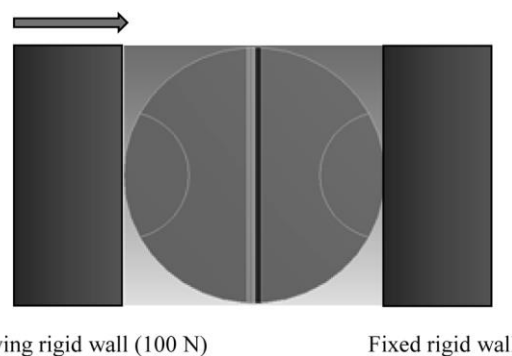As important characteristics of scored tablets, the dividing strength, halving equality, and breaking strength were determined. Figure 4 shows the apparatus for testing the dividing strength. A stainless steel probe with a triangle pole blade (a blade angle of 45° and length of 8 mm) was driven in the vertical direction until the tablets began subdividing. The score line of the tablet was mounted parallel to the direction of the blade length. The maximum force was determined as the dividing strength. The halving equality was gravimetrically evaluated by using the difference factor (F_D), defined as:

$$F_D \ (\%) = |W_A - W_B| / (W_A + W_B) \times 100 \tag{3}$$

where W_A and W_B are weights of each halves of the subdivided tablets, respectively. Theoretically, the F_D value was expressed as a value 0–100%; a smaller F_D value indicates a greater halving equality. The breaking strength of scored tablets was determined using a portable hardness tester (PC-30; Okada Seiko Co., Ltd., Tokyo, Japan). The tablet was mounted on the hardness tester ensuring that the scored line was placed orthogonally to the direction of diametrical compression.
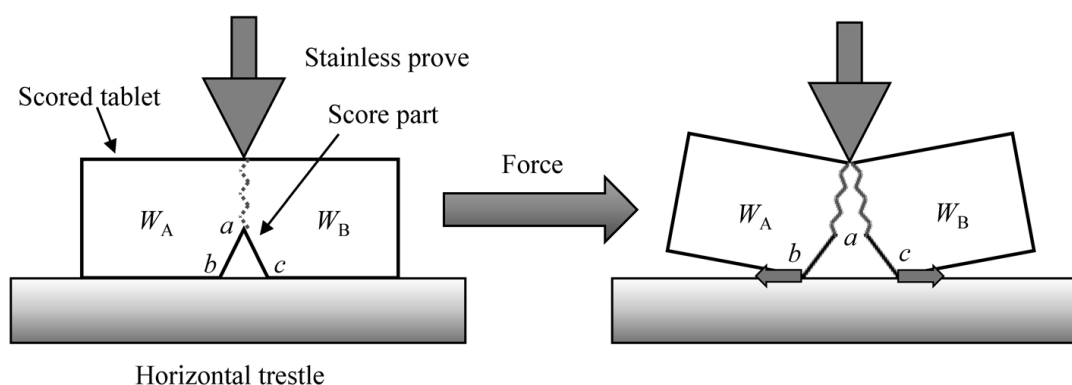
Fig. 4. Experimental Setup for Measuring Dividing Strength of Scored Tablets
The scored tablet was fixed on the horizontal trestle such that the scored area faces down. A stainless steel probe with a triangle pole blade (45° blade angle and 8 mm blade length) was driven into the tablet until the tablet began breaking. W_A and W_B are the weights of each of the halved tablets. Point b and point c move horizontally to the left and the right, respectively, after increasing the blade force. Substantial tensile stress is generated around point a with a change of tablet shape.

2.6. Computer Programs

FEM analysis of the tablet properties was performed using ANSYS® version 14.5 (ANSYS Inc., Canonsburg, PA, U.S.A.). Two-way factorial ANOVA and regression analysis were performed using JMP® version 8 (SAS Institute Inc., Cary, NC, U.S.A.).

3. Results and Discussion

3.1. Simulation of Maximum Principal Stress

FEM simulation, the scored tablet was represented as a continuum elastic model. From a stress–strain curve determined using the test formulation listed in Table 1, elastic parameters, E=2.35±0.07 GPa and v=0.08±0.01 as the mean ± standard deviation (S.D.) for three determinations, were estimated, and were used as parameters in the FEM simulation. The principal stresses were given as the stress tensor elements when the shear stress components became zero and were represented as maximum (σ_1), intermediate (σ_2), and minimum (σ_3) principal stresses. In this study, I employed the σ_1 value as a representative of the stress generated after applying the external force to the tablets. When the σ_1 value was positive, the tensile force was working at the relevant site of the tablets and *vice versa*.

3.2. Effect of Bending Force

Figure 5 shows the σ_1 value distribution on the top surface of the scored tablets after applying the bending force. Strong tensile stress was generated along the score line, and the stress increased with increasing score depth. An exceptionally large σ_1 value (*ca*. 145 MPa in Fig. 5) may be brought about by the force generated at extremely narrow area of the score tip, suggesting that the value observed with FEM simulation cannot be compared directly to the experimental results. Although the shape of score tip was set to be a fillet surface to avoid generating a singular point, the edge of V-shape notches often causes the stress concentration. Nevertheless, FEM simulation can be effectively utilized to predict experimental data on the basis of regression analysis (as I discuss later in Fig. 9). The effect of score angles on the σ_1 value was minimal. Very weak tension was generated on the other site of the top surface apart from the score line when the score was shallow (0.50–0.75 mm).

Figure 6 shows the σ_1 value distribution on the lateral surface. A tendency similar to that on the top surface was observed on the lateral surface. Strong tensile stress was generated immediately beneath the end of the score and became clear when the score was sufficiently deep (*ca*. 1.50 mm). Weak tensile force was observed around the end of the scores and the

tensile area spread depending on score depth. These results indicate that score depth is more important than score angle for the ease of subdivision and halving equality of scored tablets.
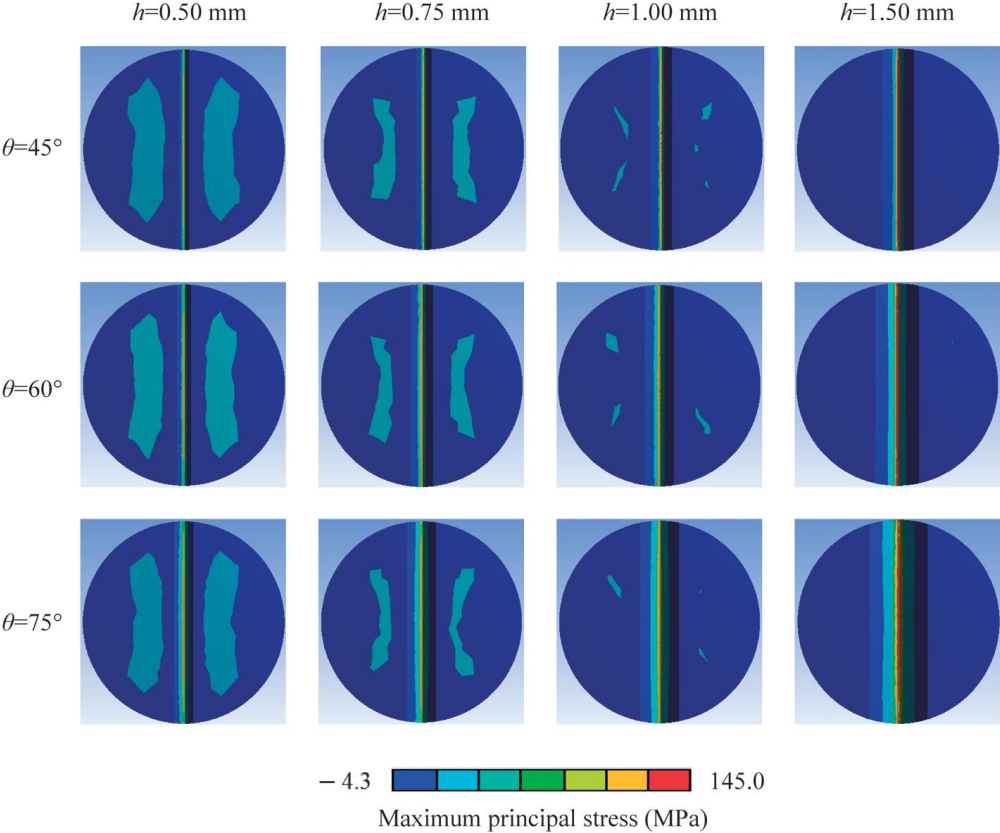

Fig. 5. The Maximum Principal Stress Distribution on the Top Surface of Scored Tablets after Applying the Bending Force
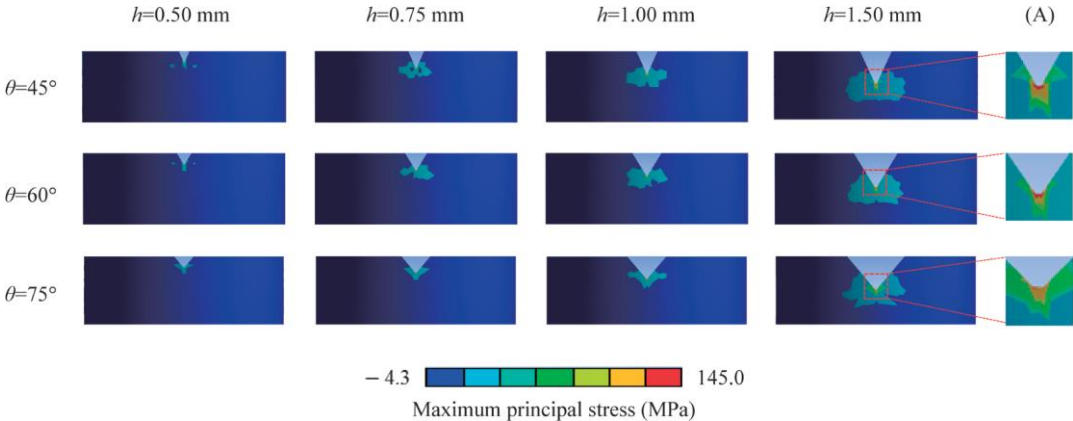*h*: score depth; *θ*: score angle.

Fig. 6. The Maximum Principal Stress Distribution on the Lateral Surface of Scored Tablets after Applying the Bending Force
h: score depth; *θ*: score angle; (A): enlarged view of the scored region at *h*=1.50 mm.

13

3.3. Effect of Diametrical Compression

Figure 7 shows the σ_1 value distribution on the top surface of scored tablets after the application of diametrical compression. Weak compression stress was observed in the limited area on the contact surface of the tablet to the rigid wall. A wide range of tensile stresses was generated on the surface in the direction of the diametrical compression axis. The area became wider as a function of score depth, but the effect of score angle was minimal. It is likely that the dominant component on the wide range of the σ_1 values is tensile strength, which works from the center to the orthogonal direction to the compression axis. Figure 8 shows the σ_1 value distribution on the lateral surface faces to the rigid moving wall. Interestingly, strong tensile stress was distributed on the center bottom as a bimodal shape, and the area was enhanced with increasing score depth. This suggests that the upper center region is compressed more easily compared with the bottom because of the existence of scores, which may lead to the generation of tensile stress on the bottom of the tablet. The sphenoidal shapes of the compressed area may reflect the bimodal shapes of tensile stress generated on the bottom area. This suggests that the tablet became more breakable with increasing score depth.

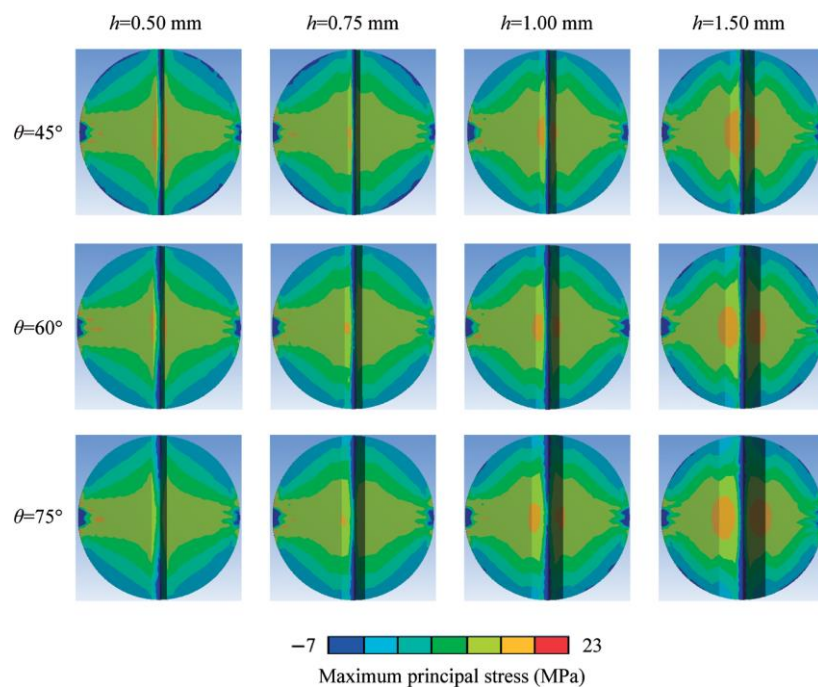Fig. 7. The Maximum Principal Stress Distribution on the Top Surface of Scored Tablets after Applying the Diametrical Direction Force
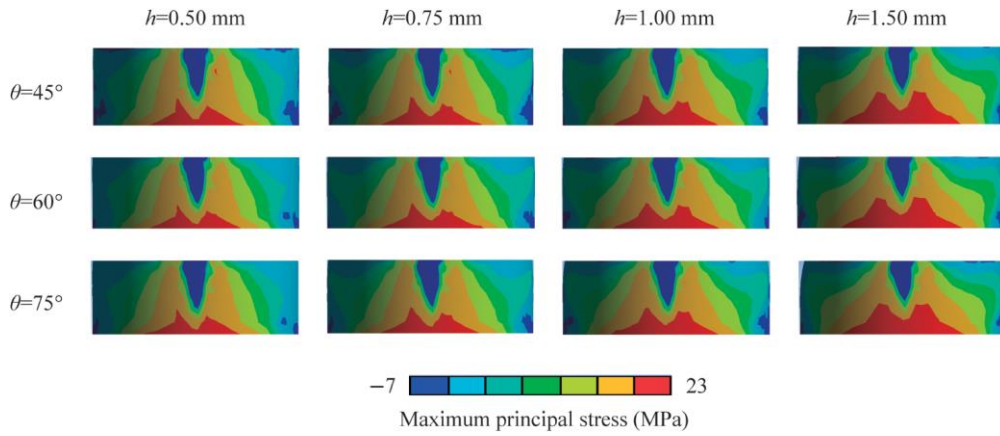h: score depth; θ: score angle.

14

Fig. 8. The Maximum Principal Stress Distribution on the Lateral Surface of Scored Tablets after Applying Diametrical Direction Force

h: score depth; *θ*: score angle. Maps show the lateral sides faced to the moving rigid wall.

3.4. Experimental Verification

As a preliminary study, an apparatus mimicking the method shown in Fig. 2 was prepared and used to measure the dividing strength of scored tablet. However, the reproducibility of the experimental result was quite poor. This is because the shape of the tablet is appreciably distorted right before the onset of breakage during the increased bending stress, and the apparatus fails to work on the tablet shape. On the other hand, a reasonable reproducibility of the dividing strength was observed by using the apparatus shown in Fig. 4. It is likely that strong tensile strength generates around the score tip with increasing blade force, and the method substantially reflects the results obtained with FEM simulation. Experimental values such as the dividing strength, halving equality (defined as F_D values), and breaking strength (hardness) are summarized in Table 2. These values were strongly dependent on the score depth and decreased with increasing depth of the score shape. In contrast, the score angle had only a minimal effect on the mechanical values. When the score shape was shallow (0.50–0.75 mm), the F_D value was extremely large and was no longer effective as a dividing line. In general, less than 1% of the F_D value is acceptable for the clinical use of subdividing tablets, in which the therapeutic dose of a drug must be strictly controlled.[31,48] A rather deep score (*ca*. 1.50 mm) was required to ensure good halving equality. However, this may lead to mechanically weak tablets, as summarized in Table 2. The dividing ease and halving equality are features opposed to the mechanical strength of the tablet. The two-way ANOVA results for the dividing strength, halving equality, and hardness are summarized in Tables 3–5, respectively. Both dividing strength and halving equality were significantly affected by the score depth (*h*) and angle (*θ*) as well as by their interaction, although the effect of score depth on these mechanical characteristics was predominant, as observed in the F_o values (Tables 3, 4). The hardness was significantly affected by the score depth only (Table 5). Figure 9 shows relationship of experimental values of dividing strength, halving equality and hardness to the maximum principal stress around the score line after applying bending force or diametrical direction force. Increasing the σ_I value resulted in the improvement of dividing ease and halving equality. But the tablet hardness weakened with increasing the σ_I value. Since the FEM simulation results

were well-correlated to the experimental results, this technique can be applied to evaluate the score shape of tablets *in silico* without the need for costly experiments.

Table 2. Dividing Strength, Halving Equality and Hardness in Scored Tablets

Depth, h (mm)	Angle, θ (°)	Dividing strength (N)	Halving equality F_D value (%)	Hardness (N)
0.50	45	79.05±1.13	57.94±0.67	33.33±1.53
0.75	45	71.21±1.13	53.83±0.66	28.00±1.00
1.00	45	63.37±2.04	3.04±0.86	25.67±1.53
1.50	45	32.99±1.50	0.66±0.04	24.00±1.00
0.50	60	70.23±2.04	55.85±0.33	32.33±0.58
0.75	60	65.66±0.98	9.69±0.34	27.33±0.58
1.00	60	61.09±1.50	2.64±0.17	25.33±1.53
1.50	60	26.79±2.26	0.35±0.33	23.67±1.15
0.50	75	60.76±1.96	53.27±0.69	31.67±0.58
0.75	75	55.53±1.13	7.68±1.55	28.33±0.58
1.00	75	51.29±1.50	3.67±0.80	26.67±1.15
1.50	75	22.87±1.13	0.83±0.33	21.33±2.08

Each datum represents the mean±S.D. for three determinations.

Table 3. Two-way ANOVA for Dividing Strength of Scored Tablets

Factor	Degrees of freedom	MS[a]	Fo[b]	p[c]
Depth, h	3	3225.90	1286.39	<0.0001
Angle, θ	2	598.76	238.77	<0.0001
$h \times \theta$	6	14.62	5.83	<0.0007
Error	24	2.51		

a) Mean square, b) Observed *F* value, c) Risk rate.

Table 4. Two-way ANOVA for Halving Equality of Scored Tablets

Factor	Degrees of freedom	MS[a]	Fo[b]	p[c]
Depth, h	3	5838.20	12501.50	<0.0001
Angle, θ	2	589.75	1262.84	<0.0001
$h \times \theta$	6	11.21	1048.60	<0.0001
Error	24	0.47		

a) Mean square, b) Observed *F* value, c) Risk rate.

Table 5. Two-way ANOVA for Hardness of Scored Tablets

Factor	Degrees of freedom	MS[a)]	Fo[b)]	p[c)]
Depth, h	3	141.88	98.22	<0.0001
Angle, θ	2	1.86	1.29	0.2941
$h \times \theta$	6	2.94	2.03	0.1005
Error	24	1.44		

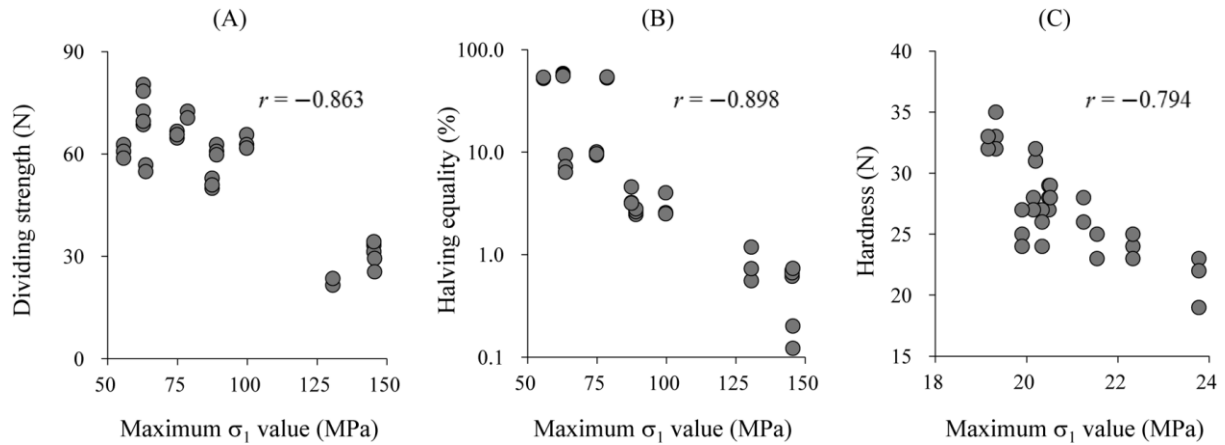a) Mean square, b) Observed F value, c) Risk rate.

Fig. 9. Relationship of Experimental Values of (A) Dividing Strength, (B) Halving Equality and (C) Hardness to the Maximum Principal Stress

4. Conclusion

FEM simulation was used to investigate the mechanical stress on the top and lateral surfaces of scored tablets after application of external forces. When a bending force was applied, strong tensile stress was generated along the score line, which increased with increasing score depth. A wide range of tensile stresses was generated on the top and lateral surfaces of scored tablets after applying diametrical compression. The area became wider as a function of score depth. A reasonable relationship between FEM simulation and experimental results was observed, suggesting that FEM simulation is advantageous for designing scored tablets. Further investigation will be needed for the quantitative prediction of pharmaceutical characteristics of scored tablets based on FEM simulation. In addition to the depth and angle of scores, other factors such as the tablet shape, thickness, and density should be taken into consideration in order to understand the details affecting the relationship between FEM simulation and experimental results. Nevertheless, FEM simulation is useful for improving the understanding of the pharmaceutical characteristics of scored tablets.

Chapter 2

Strength Simulation of Scored Tablets Based on the Finite Element Method Using an Extreme Vertices Design

1. Introduction

There is a growing expectation that the FEM can be effective in pharmaceutical design.[49,50] FEM is a numerical technique for solving complicated systems that is well known to scientists and engineers. By applying FEM, I can understand the physical behaviors of a complex object and predict the performance of a design such as the tableting process[14,15,47,50] and strength simulation.[35,51,52]

The RSM is used to model the relationships between design variables and pharmaceutical responses.[53,54] The RSM-S has been developed to determine the acceptable formulations of pharmaceutical compounds.[55] The RSM-S approach enables us to understand better the causal relationships in pharmaceutical design and to estimate a robust optimal formulation and process parameter.[56-58]

Tablets should be sufficiently strong to hold together during postcompaction operations, packaging, storage, and use. To evaluate whether tablets have sufficient strength, their hardness is measured by diametral compression during pharmaceutical development. In this test, the tablet is enclosed from both sides, and load is applied gradually. Then, tablets are crushed along their central lines. The maximum crush force is considered to be the tablet hardness. When tablets have a breaking line, large differences in stress distributions are observed, depending on the position of the line during hardness testing.[27] This consideration is important for quality control, because the position of the breaking line could lead to large increases in the variations of tablet hardness. However, the relationship between FEM results and tablet hardness has not been sufficiently validated in the past. Moreover, the influence of tablet formulation and the shape of the breaking line on stress distributions during hardness testing has not been determined. Therefore, the purpose of this study was to explore differences in stress distribution between these design variables using FEM. I also aimed to determine any relationships between FEM results and tablet hardness using RSM-S. To achieve this, I prepared 10 types of tablets by a wet granulation compression method according to the extreme vertices design and measured the elastic parameters of each type of granule. Subsequently, I simulated the mechanical strain distribution of tablets using FEM. The depths and angles of the score were

21

changed as design variables. Then, RSM-S was applied to reveal any causal relationships between design variables and strain in each tablet simulated by FEM. Finally, the relationship between strain and tablet hardness was evaluated.

2. Experimental

2.1. Materials

Lactose (LAC; Tablettose 80) was purchased from Meggle Japan Co., Ltd. (Tokyo, Japan), cornstarch (CS; Graflow M) from Nippon Starch Chemical Co., Ltd. (Osaka, Japan), and microcrystalline cellulose (MCC; Ceolus PH-101) from Asahi Kasei Chemicals Co., Ltd. (Tokyo, Japan). Low-substituted hydroxypropyl cellulose (L-HPC; LH-21) was a gift from Shin-Etsu Chemical Co., Ltd. (Tokyo, Japan). Polyvinylpyrrolidone K90 (PVP K90) was a gift from Nippon Shokubai Co., Ltd. (Osaka, Japan). Magnesium stearate (Mg– St) was purchased from Wako Pure Chemical Industries, Ltd. (Osaka, Japan).

2.2. Preparation of Granules and Scored Tablets

I accurately weighed a total quantity of 189 g of LAC, CS, and MCC, 4 g of PVP K90 as a binder, and 6 g of L-HPC as a disintegrant, and blended all excipients, with the exception of Mg–St, using a mixer (KM4005, De Longhi, Treviso, Italy) for 1 min. Purified water equivalent to 30% of the powder mixture by weight was added as the granulation liquid, and the mixture was blended using the same mixer (impeller speed, 470 rpm; blending time, 5 min). After the granulation process, the granules were sieved through a 5.8-mm mesh and dried at 75°C for 60 min. The granules were then separated using a series of sieves of 250–710 μm pore size. Mg–St (0.5% of the granule weight) was added, and the mixture was blended using a V-type mixer (S-3, Tsutsui Scientific Instruments Co., Ltd., Tokyo, Japan) for 2 min. Next, 200 mg of the final blend was compressed at 4 kN into flat-faced scored tablets, 8 mm in diameter, using a hydraulic press (Model PCH-20, NPa System Co., Ltd., Warabi, Saitama, Japan). Twelve types of scores were fabricated on the flat-faced tablets by changing the depth (h=0.50, 0.75, 1.00, and 1.50 mm) and the angle (θ=45°, 60°, and 75°).

2.3. Experimental design

Varying amounts of MCC (XI), CS ($X2$), and LAC ($X3$) in each tablet were selected as formulation factors (Table 6). The lower and upper limits of the levels of each factor were set as follows.

$$57 \leq X_1 \leq 132 \text{ (mg)} \tag{4}$$

$$0 \leq X_2 \leq 132 \text{ (mg)} \tag{5}$$

$$0 \leq X_3 \leq 132 \text{ (mg)} \tag{6}$$

$$X_1 + X_2 + X_3 = 189 \text{(mg)}. \tag{7}$$

Therefore, the feasible experimental region in the simplex lattice design had a trapezoidal shape. The formulation factors were assigned and prepared according to an extreme vertices design, including a duplicate of the centroid.[59]

Table 6. Quantities of MCC, CS, and LAC for tablets based on an extreme vertices design.

Formulation	MCC (X_1 (mg))	CS (X_2 (mg))	LAC (X_3 (mg))
1	132.09	56.61	0
2	132.09	0	56.61
3	56.61	132.09	0
4	56.61	0	132.09
5	132.09	28.31	28.31
6	94.35	94.35	0
7	56.61	66.05	66.05
8	94.35	0	94.35
9	94.35	47.18	47.18
10	94.35	47.18	47.18

2.4. Determination of Elastic Parameters

Young's modulus (E) and Poisson rate (v) were determined from the unloading curve of a die compaction experiment. The axial upper/lower punch forces and displacements and the radial die-wall pressure were measured during compaction using an instrumented hydraulic press (TK-TB20KN, Tokushu Keisoku Co., Ltd., Yokohama, Japan). The E and v values were calculated based on the variation of axial stress with volume strain (ε_Z) and the stress path during the compaction of granules. The stress path is shown by a scatter plot in which the x and y-axes show the equivalent hydrostatic pressure stress (p) and the square root of the second invariant of the deviatoric stress ($\sqrt{J'_2}$) plane, respectively. The ε_Z value was defined as a ratio of the powder height during compaction (Z) to Z_0: $\varepsilon_Z = |ln(Z/Z^0)|$.[46] The bulk modulus K and shear modulus G were defined as:

$$K + \frac{4}{3}G = \frac{(\sigma_z^m - \sigma_z^h)}{(\varepsilon_z^m - \varepsilon_z^h)} \tag{8}$$

$$\frac{2G}{\sqrt{3}K} = \frac{\sqrt{J_2'^m}}{p^m - p^h} \tag{9}$$

where the superscripts m and h denote the values at points when the compression pressure indicates the maximum value and $\sqrt{J'_2}$ is 0, respectively. Knowing the K and G values, the E and v values can be determined from the following.

$$E = \frac{9GK}{3K + G} \tag{10}$$

$$v = \frac{3K - 2G}{2(3K + G)} \tag{11}$$

Excellent descriptions of measuring E and v have been published.[21,47]

2.5. FEM Simulation

In the initial stage of loading the external force to the tablet, I hypothesized that the tablet could be represented as a continuum in an elastic model. Although the elastic parameter is

varied as a function of tablet density,[14] it was considered as a constant value in this study. This continuum elastic model has been used widely in the simulation of diametral compression, and the results obtained are reasonable.[27,60] The FEM was applied to estimate the principal stresses generated at the top and lateral surfaces and along the scored lines of the tablets. To avoid generating a singular point, the shape of the score tip was set to be a fillet surface. Strain distribution was simulated after the application of external forces such as a bending stress and diametral compression. The methods for application of these external stresses to the scored tablet are illustrated schematically in Fig. 10. The scored tablet was compressed against a rigid wall by moving the other side horizontally at 100 N, and the angles of the scored line to the diametral compression axis were set at 0°, 45°, or 90°. Strain distributions on the top surface were estimated using the FEM simulation.
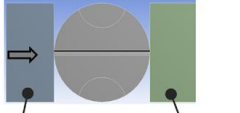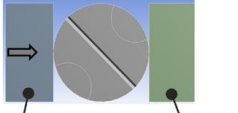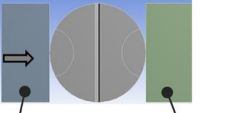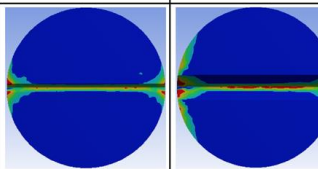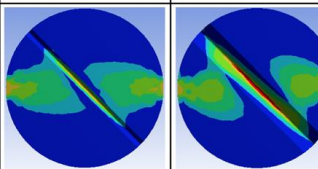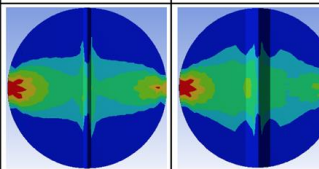

Score line	0°		45°		90°	
Method of FEM simulation	Moving rigid wall (100 N) Fixed rigid wall		Moving rigid wall (100 N) Fixed rigid wall		Moving rigid wall (100 N) Fixed rigid wall	
Score depth, h (mm)	0.50	1.50	0.50	1.50	0.50	1.50
Result of FEM simulation						
Experimental results						

Fig. 10. Method for Applying the Diametral Compression to Scored Tablets and Change of Distribution of Maximum Principal Strain Brought about by the Direction of the Score Line

The right rigid wall was fixed and faced the side of the tablet. The tablet was compressed by moving the left rigid wall horizontally at 100 N, and the angle of the scored line to the diametral compression axis was set at 0°, 45°, or 90°. The score angle was set at 45° in this figure.

2.6. Determination of Tablet Characteristics

The breaking strength of scored tablets and tablet hardness were determined using a portable hardness checker (PC-30, Okada Seiko Co., Ltd., Tokyo, Japan). The tablet was mounted on the checker, and the angles of the scored line to the diametral compression axis were set at 0°, 45°, or 90°.

2.7. Computer programs

The FEM analysis of the tablet property was performed using ANSYS[®] version 16.0 (ANSYS Inc., Canonsburg, PA, U.S.A.). The RSM-S was applied to generate response surfaces and was performed using data NESIA[®] version 3.2 (Azbil Corporation, Fujisawa, Japan).

3. Results and Discussion

3.1. Simulation of Diametral Compression

To perform FEM simulation, the scored tablet was represented as a continuum elastic model. The Young's modulus (E) and Poisson rate (v) of the test formulations were calculated from the stress–strain curve during the tableting process. These parameters, summarized in Table 7, were fed into a computer for the FEM simulation. The principal strains are defined as the strain tensor elements when the three-dimensional strain coordinate is rotated so that the shear strain components become zero. They are represented as maximum (ε_1), intermediate (ε_2), and minimum (ε_3) principal strains. In this study, I employed the ε_1 value as representative of the strain generated after applying an external force to the tablets. Generally, when elastic model is applied, strains are correlated with external force and tablet does not break in FEM analysis. In the preliminary test, it was confirmed that when an external force was set at lower than 100 N, similar tendency was obtained although absolute values varied by an external force.

Typical examples of the distribution of ε_1 values estimated by the breaking strength simulation are shown in Fig. 10. When the angle of the scored line to the breaking force was set at 90°, the horizontal strain increased. Turning the angle of the scored line to 45° resulted in an ε_1 value being generated along the scored line. As the score depth increased, this tendency increased. It is likely that the potential strain generated along the scored line is closely related to the breaking strength of the tablets. When the angle of the scored line was changed to 0°, a very strong ε_1 value appeared only on the scored line. Similar phenomena were seen regardless of differences in the score depth, although the absolute value of the strain on the scored line increased with increasing score depth. The strain decreased markedly when the angles of the scored line to the diametral compression axis were changed to 45° and 90°. These findings coincided fairly well with the results reported by Podczeck et al.[27,61] who suggested that considerable differences in stress distribution appeared depending on the angle of the scored line to the diametral compression axis. The stress values at failure were predicted to be similar for tablets tested at an angle of 45° or above, whereas at lower test angles, the predicted breaking

28

loads were up to three times greater. Comparisons of FEM simulations with actual experiments are described in the next section.

To visualize the relationships between the ε_1 values and various factors, the response surfaces for the ε_1 values were estimated by RSM-S. Figures 11a and 11b show the ε_1 values of Rp. 1 modeled as a function of the angle of the scored line to the compression axis, the score angle, and the score depth. The response surface showed that the ε_1 value was strongly dependent on the angle of the score line to the compression axis and deceased as the angle increased from 0° to 45° to 90°. The ε_1 value was also affected by the score angle (Fig. 11a) and the score depth (Fig. 11b). The ε_1 value increased with increasing score angle and score depth.

Figure 12 shows the response surface on which the ε_1 was modeled as a function of formulation factors when the angle of the scored line to the compression axis, the score angle, and the score depth were set at 45°, 60°, and 0.75 mm, respectively. The maximum ε_1 value was obtained with Rp. 3, which contained a large amount of CS, in all scored line positions. In contrast, the ε_1 value of Rp. 2, which contained a large amount of MCC, was minimal. It is considered that the strain in Rp. 3 was the highest because it had the smallest value for the Young's modulus. Although Figs. 11 and 12 show typical examples, similar results were obtained from the other formulations and conditions.

Table 7. Elastic Modules of All Formulations

Formulation	Young's modules (GPa)	Poisson rate
1	2.95± 0.06	0.1624± 0.0019
2	4.13± 0.06	0.1492± 0.0010
3	2.03± 0.00	0.1454± 0.0001
4	3.48± 0.05	0.1621± 0.0152
5	3.43± 0.04	0.1679± 0.0197
6	2.56± 0.03	0.1605± 0.0019
7	2.73± 0.08	0.1354± 0.0050
8	3.81± 0.09	0.1807± 0.0246
9	2.80± 0.02	0.1543± 0.0114
10	2.76± 0.04	0.1562± 0.0030

Each value represents the mean±S.D. for three determinations.

(a)   (b)
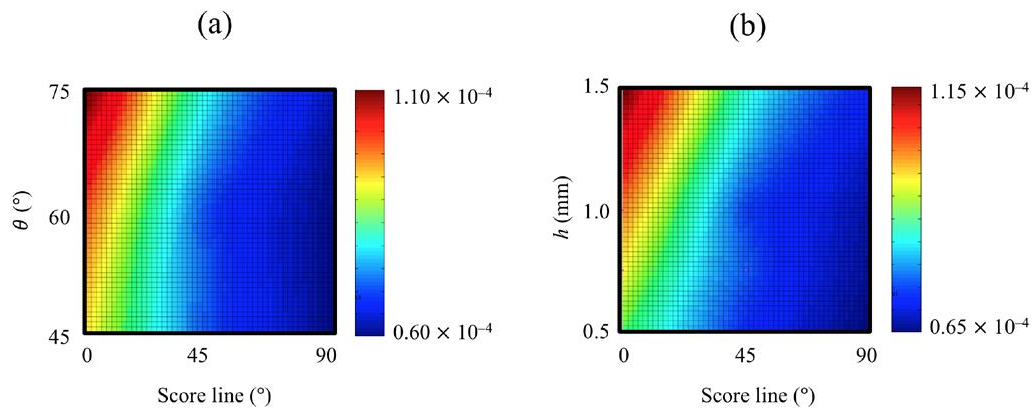
Fig. 11. Response Surface of ε1 Values Generated by RSM-S for Rp. 1
The ε_1 values were modeled as a function of the angle of the score line to the compression axis, the score angle, and the score depth. (a) The x and y axes represent the angles of the score line to the compression axis and score angle, respectively, and the score depth was set at 1.0 mm. (b) The x and y axes represent the angles of the score line to the compression axis and score depth, respectively, and the score angle was set at 60°. θ, score angle; h, score depth.
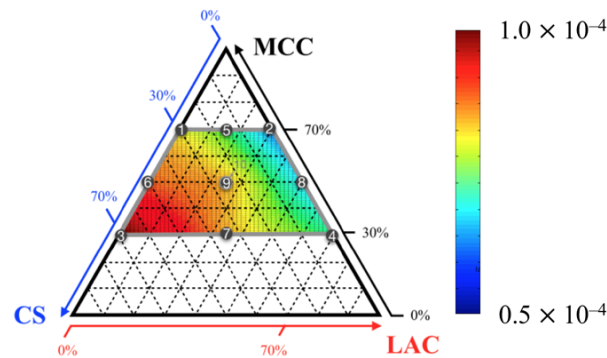
Fig. 12. Response Surface of ε_l Values Generated by RSM-S as a Function of Formulation Factors

Geometric representation of the extreme vertices design for three components. Ten formulations were assigned as vertices, as center points between vertices, and as centroids. Each number indicates formulation numbers, respectively. The angle of the score line to the compression axis, the score angle, and score depth values were set at 45°, 60°, and 0.75 mm, respectively.

3.2. Experimental Validation of FEM Simulation

The lowest rows in Fig. 10 show the breaking behaviors for three test angles of the scored tablets. The experimental results were similar to those of the simulations. When the angle of the scored line to the diametral compression axis was 0°, regardless of the depth and angle of the score, the cracks appeared to initiate at the scored line in the direction of compression. When the angle of the scored line was changed to 45° at a score depth of 0.50 mm, the cracks propagated in the direction of compression. In contrast, with a score depth of 1.50 mm, the cracks not only appeared in the direction of the compression but also approached the score line. A similar tendency was observed when the score angle was much wider. When the angle of the scored line to the diametral compression axis was changed to 90°, regardless of the score shape, horizontal cracks appeared on the compression axis.

To compare the relationships between the ε_l value and tablet hardness, the response surface of tablet hardness was estimated using RSM-S.

Typical examples are shown in Fig. 13. When the angle of the scored line to the diametral compression axis was 0°, the breaking strength indicated lower values, whereas at 90°, it showed higher values. Furthermore, as the depth of the score decreased, it was demonstrated

31

that the scored line direction had more impact. In comparison to the results of direct compression (Table 2), for all formulations except Formulation 3, the tablets produced using wet granulation had higher breaking strengths. This is thought to be due to improved flowability, tableting and inter-particle cohesion as a result of wet granulation. For all score shapes, a tendency was observed for higher MCC content ratios to show higher breaking strength values. This may be due to MCC acting as a binder with excellent compression formability.

To investigate the quantitative relationships between ε_1 values and tablet hardness, a scatter plot was made using 360 types, with differences in the formulations, the angles of the score line to the compression axis, the score angles, and the score depths (Fig. 14). Regression analysis revealed that the correlation coefficient of the power equation (r=0.724) was better than those of linear (r=0.667), polynomial (r=0.719), and exponential equations (r=0.711). Outliers, which might be derived from errors in the FEM analysis, were excluded from regression analyses. The best fitting power equation was as follows.

$$Tablet\ hardness = 0.0101\varepsilon_1{}^{-1.6379}$$

This result revealed that the least deformable tablet had the greatest hardness. Therefore, this result is considered to be reasonable, although a large variation was observed in the regression analyses. Such regression errors might arise from a simple FEM model because each tablet was considered as a uniform elastic model in this study regardless of whether the tablet's inner structure—such as density and stress distribution— was inhomogeneous.[14] Moreover, although the ε_1 was considered as an explaining variable in this study, multivariate analysis—in which all strains of inner tablet are considered as explaining variables—could increase prediction accuracy.[41,45] These approaches might enable us to predict *in silico* tablet hardness of arbitrary formulation and shape accurately.

(a) 45 °-0.5 mm

0°

MCC

CS   LAC

6   Breaking strength   88
(N)

45°

MCC

CS   LAC

6   Breaking strength   88
(N)

90°

MCC

CS   LAC

6   Breaking strength   88
(N)

(b) 45 °-1.0 mm

0°

MCC

CS   LAC

6   Breaking strength   88
(N)

45°

MCC

CS   LAC

6   Breaking strength   88
(N)

90°

MCC

CS   LAC

6   Breaking strength   88
(N)

(c) 45 °-1.5 mm

0°

MCC

CS   LAC

6   Breaking strength   88
(N)

45°

MCC

CS   LAC

6   Breaking strength   88
(N)

90°

MCC

CS   LAC

6   Breaking strength   88
(N)
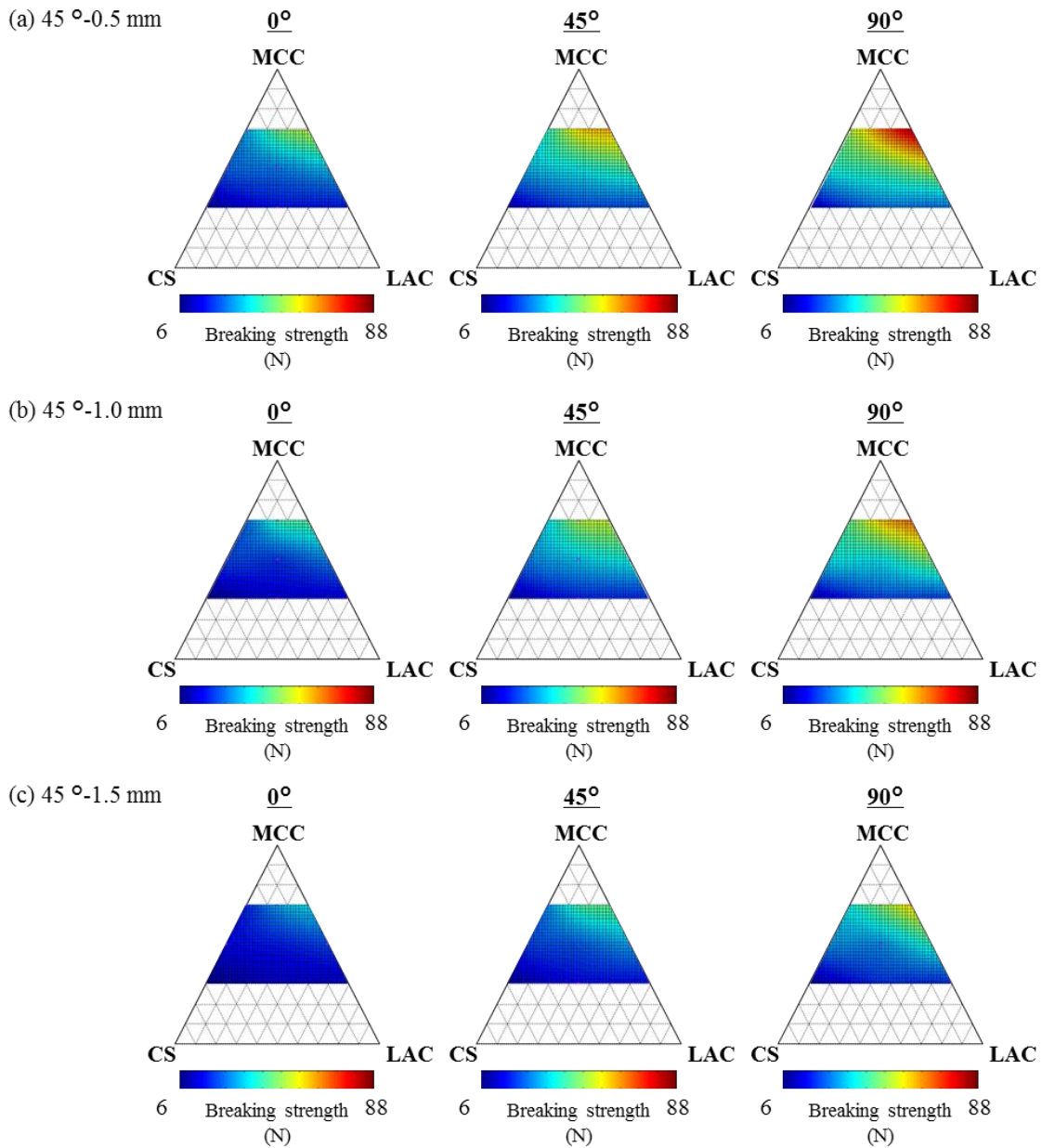
Fig. 13. Response surfaces for breaking strength as a function of quantity ratios of MCC, CS and LAC. Scored shape (a) 45 °- 0.5 mm, (b) 45 °- 1.0 mm, (c) 45 °- 1.5 mm. Angle of dividing line to the breaking force : 0 °, 45 °, 90 °.
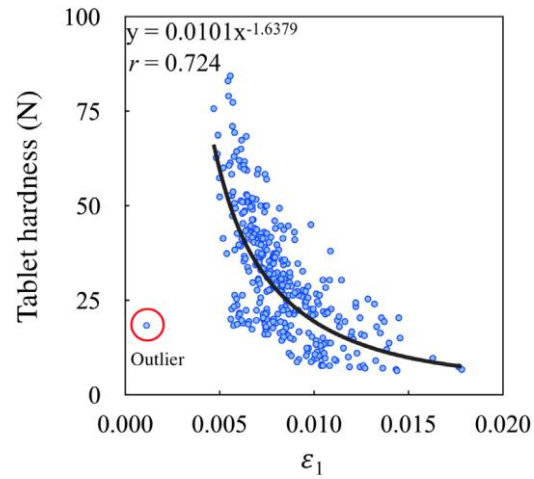
Fig. 14. Correlation of ε_1 Values Calculated by FEM Simulation with Tablet Hardness

Three hundred sixty samples, with differences in formulation, angles of the score line to the compression axis, score angles, and score depths, were used. Outliers were excluded from the regression analysis.

4. Conclusion

I investigated the mechanical strain on the top surface of scored tablets after application of external forces by using the FEM simulation. For diametral compression, considerable differences were observed in the strain distribution, depending on the angle of the score line to the diametral compression axis: 0°, 45°, or 90°. The strain values increased with increasing score depth. The FEM simulation was validated by the experimental data. Moreover, I found that the value of ε_l obtained from FEM simulation was negatively correlated with tablet hardness, suggesting that the FEM simulation was advantageous for designing scored tablets. I conclude that such FEM simulation is useful for achieving an objective understanding of the pharmaceutical characteristics of scored tablets.

Summary

Pharmaceutical dosage forms include tablets, granules, and capsules. Tablets are preferred by patients due to their ease of use and portability. Many factors can affect the quality of the drug product because tablets are composed of a variety of factors in the formulation and manufacturing process. Therefore, understanding of these cause relationships is required in formulation development. However, quantitative formulation design is considered difficult, and formulation development has been biased toward subjective and empirical judgments.

In recent years, the "QbD" concept was proposed in the ICH Q8 guidance and the establishment of a science-based rationale and a design space in pharmaceutical formulation development is desired.

Therefore, many simulation methods have been developed to model the compaction behavior of powders and the fluidized bed granulation process, and to understand the important factors that affect formulation quality. However, the model formulation and shape which lack practicality are used, the simulation was only validated experimentally, and no studies have examined the causal relationship between the simulation results and the quality attribute.

The purpose of this study is to establish that the FEM, a form of CAE simulation, is a useful tool for understanding important factors in formulation development.

In chapter 1, the aim of this study was to clarify the effect of score shapes on the essential characteristics of tablets by using FEM simulation. I only focused on the depth and angle of scores in this study as the starting point for the potential use of FEM simulation for the design of scored tablets. A runnel of triangle pole on the top surface of flat tablets was fabricated as the score shape. The depth and angle of scores were changed as design variables. The scored tablet was manufactured by direct compression method, and the simulation and experiment were verified. The scored tablet was manufactured by direct compression method, and the simulation and experiment were verified. The results of bending force showed that the shallower score shape, the smaller stress generated in along the score line and the strain was generated in along other than the score line. As strong tensile stress was generated along the

score line, which increased with increasing score depth. A wide range of tensile stresses was generated on the top and lateral surfaces of scored tablets after applying diametrical compression. The area became wider as a function of score depth, but the effect of score angle was minimal. A reasonable relationship between FEM simulation and actual experimental results was observed.

In chapter 2, the purpose of this study was to explore differences in stress distribution between these design variables using FEM. I also aimed to determine any relationships between FEM results and tablet hardness using RSM-S. To achieve this, I prepared 10 types of tablets by a wet granulation compression method according to the extreme vertices design and measured the elastic parameters of each type of granule. Subsequently, I simulated the mechanical strain distribution of tablets using FEM. In the breaking strength simulation, when the angle of the scored line to the breaking force was set at 90°, the horizontal strain increased. Turning the angle of the scored line to 45° resulted in the strain being generated along the scored line. As the score depth increased, this tendency increased. When the angle of the scored line was changed to 0°, a very strong ε_1 value appeared only on the scored line. Similar phenomena were seen regardless of differences in the score depth, although the absolute value of the strain on the scored line increased with increasing score depth. The experimental results in the breaking behaviors for three test angles of scored tablets showed that as the depth and angle of scored line increased, cracks were observed to form along the scored line. When the angle of the scored line to the diametral compression axis was changed to 90°, regardless of the score shape, horizontal cracks appeared on the compression axis. The experimental results were similar to breaking strength simulations.

Furthermore, I found that the value of ε_1 obtained from FEM simulation was negatively correlated with tablet hardness, suggesting that the FEM simulation was advantageous for designing scored tablets.

The results of the above studies indicate that the halving equality of scored tablets is affected by the physical properties of the powder, the manufacturing conditions, and the shape of the

score. Therefore, it is necessary to take these factors into consideration when designing a formulation for the production of scored tablets. The more uniform the dividing strength of the scored tablet, the greater the dividing strength, and a proper balance must be achieved.

The results of these studies show that FEM is similar to actual physical behavior and can predict the quality characteristics of formulations containing many formulation factors. Future development of FEM simulation is expected to improve tableting failure and shorten the development time of tablet shapes. When tableting problems occur, stable production is not possible and the development timeline needs to be delayed. If this occurs during commercial production, in the worst case scenario, it can lead to serious problems such as not being able to supply medicinal products to patients. Therefore, measuring residual stress distribution in the tableting process by FEM simulation is expected to reduce tableting failures. The material of the punches and die is metal, and it takes about two months from the time an order for a candidate shape is placed to the time it is received. In addition, it is necessary to repeat a trial-and-error process of making one punch, making a tablet and evaluating the quality before determining the tablet shape, which takes a lot of time and costs. Therefore, the use of FEM simulation is expected to shorten the development period and reduce development costs. FEM simulations suggest that it is possible to identify important factors and it is useful tools to accelerate the formulation development process.

Acknowledgements

First of all, I would like to express my gratitude and deepest appreciation to Professor Kozo Takayama for his guidance and advice in my research work and preparing this dissertation.

Secondly, I would like to also express my great appreciation to Professor Yasuko Obata and Professor Yoshinori Onuki for their helpful guidance and assistance in my research work.

Also, I wish to thank Dr. Yoshihiro Hayashi, Ms. Saori Otoguro (Department of Pharmaceutics, Hoshi University), Mr. Takahiro Miura (Cybernet Systems Co., Ltd.,) for their valuable suggestions and fruitful discussions.

In addition, I am grateful to Mr. Teppei Shimizu, Ms. Chihiro Kida, Mr. Naoto Uehara and all my colleagues of the Department of Pharmaceutics of Hoshi University for their kindness and assistance.

Finally, I wish to express my sincere gratitude to my wife, son, parents and sister. This thesis would not have been fulfilled without their encouragement and support of my study and life.

References

1. Gohel, M., Jogani, P. Functionality testing of a multifunctional directly compressible adjuvant containing lactose, polyvinylpyrrolidone, and croscarmellose sodium. *Pharm. Technol.,* 26, 64-82 (2002).

2. Pavliv, L., Cahill, J. F. Formulation and Manufacturing, in *Drug and Biological Development: From Molecule to Product and Beyond* (ed. Evens, R. P.) 202-221 (New York, Springer US, 2007).

3. Sedo, K., Kararli, T. Global report-2018 global drug delivery & formulation report: Part 1, a global review. *Drug Dev Deliv.*, 2019.

4. Kritensen, H. G., Schaefer, T. Granulation: A Review on Pharmaceutical WetGranulation, *Drug Dev. Ind. Pharm.*, 13, 803-872 (1987).

5. Otsuka, T., Iwao, Y., Miyagishima, A., Itai, S. Application of principal component analysis enables to effectively find important physical variables for optimization of fluid bed granulator conditions, *Int. J. Pharm.*, 409, 81-88 (2011).

6. Pandey, P., Badawy, S. A quality by design approach to scale-up of high-shear wet granulation process. *Drug. Dev. Ind. Pharm.*, 42, 175-189 (2016)

7. Shi, L., Feng, Y., Sun, C. C. Massing in high shear wet granulation can simultaneously improve powder flow and deteriorate powder compaction: A double-edged sword, *Eur. J. Pharm. Sci.*, 43, 50-56 (2011).

8. Leitritz, M., Krumme, M., Schmidt, P. C. Force-curves of a rotary tablet press. Interpretation of three compressibility of a modified starch containing various amounts of moisture, *J. Pharm. Pharmacol.,* 48, 456-462 (1996).

9. Rojas, J., Buckner, I., Kumar, V. Co-processed excipients with enhanced direct compression functionality for improved tableting performance, *Drug Development and Industrial Pharmacy.,* 38, 1159-1170 (2012).

10. Maurer, L., Leuenberger, H. Terahertz pulsed imaging and near infrared imaging to monitor the coating process of pharmaceutical tablets, *Int. J. Pharm.,* 370, 8-16 (2009).

11. International Conference on Harmonization of Technical Requirements for Registration of Pharmaceuticals for Human Use (August 2009). Pharmaceutical Development - Q8 (R2). http://www.ich.org/products/guidelines/quality/article/ quality-guidelines.html

12. International Conference on Harmonization of Technical Requirements for Registration of Pharmaceuticals for Human Use (November 2005). Quality Risk Management - Q9.

http://www.ich.org/products/guidelines/quality/article/ quality-guidelines.html

13. International Conference on Harmonization of Technical Requirements for Registration of Pharmaceuticals for Human Use (June 2008). Pharmaceutical Quality System - Q10. http://www.ich.org/products/guidelines/quality/article/ quality-guidelines.html

14. Cunningham, J. C., Sinka, I. C., Zavaliangos, A. J. Analysis of tablet compaction. I. Characterization of mechanical behavior of powder and powder/tooling friction, *J. Pharm. Sci.,* 93, 2022-2039 (2004).

15. Michrafy, A., Diarra, H., Dodds, J. A., Michrafy, M., Penazzi, L. Analysis of strain stress state in roller compaction process, *Powder Technol.,* 208, 417-422 (2011).

16. Siepmann, J., Siepmann F. Mathematical modeling of drug dissolution, *Int J Pharm.,* 453, 12-24 (2013).

17. Bai, G., Armenante, P. M. Hydrodynamic, mass transfer, and dissolution effects induced by tablet location during dissolution testing, *J. Pharm. Sci.,* 98, 1511-1531(2009).

18. Hayashi, K., Watano, S. Novel population balance model for granule aggregation and breakage in fluidized bed granulation and drying, *Powder Technology.,* 342, 664-675 (2019).

19. Hayashi, K., Nakamura, H., Watano, S. Numerical study on granule aggregation and breakage in fluidized bed granulation by a novel PBM with DEM-CFD coupling approach, *Powder Technology.,* 360, 1321-1336 (2020).

20. Rajniak, P., Stepanek, F., Dhanasekharan, K., Fanc, R., Mancinelli, C., Chern, R. T. A combined experimental and computational study of wet granulation in a Wurster fluid bed granulator, *Powder Technology.,* 189, 190-201 (2009).

21. Wu, C. Y., Ruddy, O. M., Bentham, A. C., Hancock, B. C., Best, S. M., Elliott, J.A., Modelling the mechanical behaviour of pharmaceutical powders during compaction, *Powder Technol.,* 152, 107-117 (2005).

22. Wu, C. Y., Hancock, B. C., Mills, A., Bentham, A. C., Best, S. M., Elliott, J. A., Numerical and experimental investigation of capping mechanisms during pharmaceutical tablet compaction, *Powder Technol.,* 181, 121-129 (2008).

23. Kimber, J. A., Kazarian, S.G., Štěpánek, F. Formulation design space analysis for drug release from   swelling polymer tablets, *Powder Technol.,* 236, 179-187 (2013).

24. Kimber, J. A., Kazarian, S.G., Štěpánek, F. Modelling of pharmaceutical tablet swelling and dissolution using discrete element method, *Chem Eng Sci.*, 69, 394-403 (2012).

25. Kimber, J. A., Kazarian, S.G., Štěpánek, F. DEM simulation of drug release from structurally heterogeneous swelling tablets, *Powder Technol.,* 248, 68-76 (2013).

26. Ketterhagen, W. R., Am Ende, M. T., Hancock, B. C. Process modeling in the pharmaceutical industry using the discrete element method, *J Pharm Sci.,* 98, 442-470 (2009).

27. Podczeck, F., Newton, J. K., Fromme, P. Theoretical investigations into the influence of the position of a breaking line on the tensile failure of flat, round, bevel-edged tablets using finite element methodology (FEM) and its practical relevance for industrial tablet strength testing, *Int. J. Pharm.*, 477, 306-316 (2014).

28. van der Steen K, C., Frijlink H, W., Schipper M, A., Barends D, M. Prediction of the Ease of Subdivision of Scored Tablets from Their Physical Parameters, *AAPS PharmSciTech.*, 11, 126-132 (2010).

29. Jacques E, R., Alexandridis P. Tablet Scoring: Current Practice, Fundamentals, and Knowledge Gaps, *Appl, Sci*., 9, 3066 (2019).

30. McDevitt J, T., Gurst A, H., Chen Y. Accuracy of tablet splitting, *Pharmacotherapy.,* 18, 193-197 (1998).

31. van Santen, E., Barends, D. M., Frijlink, H. W. Breaking of scored tablets: a review, *Eur. J. Pharm. Biopharm.*, 53, 139-145 (2002).

32. Rodenhuis, N., De Smet, P. A. G. M., Barends, D. M. The rationale of scored tablets as dosage form, *Eur. J. Pharm. Sci.*, 21, 305-308 (2004).

33. Sovány, T., Kása, P. Jr., Pintye-Hódi, K. Comparison of the Halving of Tablets Prepared with Eccentric and Rotary Tablet Presses, *AAPS PharmSciTech.*, 10, 430-436 (2009).

34. Sato, H., Miura, T., Furuichi, H. FEM Analysis of Tablet Hardness and Punch Strength Using ANSYS Software, *J. Comput. Sci. Tech.*, 5, 120-132 (2011).

35. Podczeck, F., Drake, K. R., Newton, J. M. Investigations into the tensile failure of doubly-convex cylindrical tablets under diametral loading using finite element methodology, *Int. J. Pharm.*, 454, 412-424 (2013).

36. Shang, C., Sinka, I. C., Pan, J. Modelling of the break force of tablets under diametrical compression, *Int. J. Pharm.,* 445, 99-107 (2013).

37. Shang, C., Sinka, I. C., Jayaraman, B., Pan, J. Break force and tensile strength relationships for curved faced tablets subject to diametrical compression, *Int. J. Pharm.,* 442, 57-64 (2013).

38. Diarra, H., Mazel, V., Busignies, V., Tchoreloff, P. FEM simulation of the die compaction of pharmaceutical products: Influence of visco-elastic phenomena and comparison with experiments, *Int. J. Pharm.,* 453, 389-394 (2013).

39. Sinha, T., Curtis, J. S., Hancock, B. C., Wassgren, C. A study on the sensitivity of Drucker–

Prager Cap model parameters during the decompression phase of powder compaction simulations, *Powder Technol.,* 198, 315-324 (2010).

40. Sinha, T., Bharadwaj, R., Curtis, J. S., Hancock, B. C., Wassgren, C. Finite element analysis of pharmaceutical tablet compaction using a density dependent material plasticity model, *Powder Technol.,* 202, 46-54 (2010).

41. Hayashi, Y., Miura, T., Shimada, T., Onuki, Y., Obata, Y., Takayama, K. Prediction of Tablet Characteristics from Residual Stress Distribution Estimated by the Finite Element Method, *J. Pharm. Sci.,* 102, 3676-3686 (2013).

42. Hayashi, Y., Otoguro, S., Miura, T., Onuki, Y., Obata, Y., Takayama, K. Effect of Process Variables on the Drucker–Prager Cap Model and Residual Stress Distribution of Tablets Estimated by the Finite Element Method, *Chem. Pharm. Bull.,* 62, 1062-1072 (2014).

43. Podczeck, F. Methods for the practical determination of the mechanical strength of tablets— From empiricism to science, *Int. J. Pharm.,* 436, 214-232 (2012).

44. Furukawa, R., Chen, Y., Horiguchi, A., Takagaki, K., Nishi, J., Konishi, A., Shirakawa, Y., Sugimoto, M., Narisawa, S. Numerical evaluation of the capping tendency of microcrystalline cellulose tablets during a diametrical compression test, *Int. J. Pharm.,* 493, 182-191 (2015).

45. Otoguro, S., Hayashi, Y., Miura, T., Uehara, N., Utsumi, S., Onuki, Y., Obata, Y., Takayama, K. Numerical Investigation of the Residual Stress Distribution of Flat-Faced and Convexly Curved Tablets Using the Finite Element Method, *Chem. Pharm. Bull.,* 63, 890-900 (2015).

46. Aydin, I., Briscoe, B. J., Sanlitűrk, K. Y. The internal form of compacted ceramic components: a comparison of a finite element modelling with experiment, *Powder Technol.,* 89, 239-254 (1996).

47. Micrafy, A., Ringenbacher, D., Tchoreloff, P. Modelling the compaction behaviour of powders: application to pharmaceutical powders, *Powder Technol.,* 127, 257-266 (2002).

48. Arruabarrena, J., Coello, J., Maspoch, S. Raman spectroscopy as a complementary tool to assess the content uniformity of dosage units in break-scored warfarin tablets, *Int. J. Pharm.,* 465, 299-305 (2014).

49. Han, L. H., Elliott, J. A., Bentham, A. C., Mills, A., Amidon, G. E., Hancock, B. C. A modified Drucker-Prager Cap model for die compaction simulation of pharmaceutical powders, *Int. J. Solids Struct.,* 45, 3088-3106 (2008).

50. Sinka, I. C., Cunningham, J. C., Zavaliangos, A. Analysis of tablet compaction. II. Finite element analysis of density distributions in convex tablets, *J. Pharm. Sci.,* 93, 2040-2053

(2004).

51. Mazel, V., Diarra, H., Busignies, V., Tchoreloff, P. Study of the Validity of the Three-Point Bending Test for Pharmaceutical Round Tablets Using Finite Element Method Modeling, *J. Pharm. Sci.,* 103, 1305-1308 (2014).

52. Mazel, V., Guerard, S., Croquelois, B., Kopp, J. B., Girardot, J., Diarr,a H., Busignies, V., Tchoreloff, P. Reevaluation of the diametral compression test for tablets using the flattened disc geometry, *Int. J. Pharm.,* 513, 669-677 (2016).

53. Huang, Y.-B., Tsai, Y.-H., Yang, W.-C., Chang, J.-S., Wu, P.-C. Optimization of Sustained-Release Propranolol Dosage form Using Factorial Design and Response Surface Methodology, *Biol. Pharm. Bull.,* 27, 1626-1629 (2004).

54. Giry, K., Viana, M., Genty, M., Wüthrich, P., Chulia, D., Wüthrich, P., Chulia, D. Surface responses and desirability functions to determine optimal granulation domains, *Drug Dev. Ind. Pharm.,* 36, 1016-1026 (2010).

55. Takayama, K., Obata, Y., Morishita, M., Nagai, T. Multivariate spline interpolation as a novel method to optimize pharmaceutical formulations, *Pharmazie,* 59, 392-395 (2004).

56. Obata, Y., Ashitaka, Y., Kikuchi, S., Isowa, K., Takayama, K. A statistical approach to the development of a transdermal delivery system for ondansetron, *Int. J. Pharm.,* 399, 87-93 (2010).

57. Onuki, Y., Morishita, M., Takayama, K. Formulation optimization of water-in-oil-water multiple emulsion for intestinal insulin delivery, *J. Control. Release,* 97, 91-99 (2004).

58. Hayashi, Y., Oshima, E., Maeda, J., Onuki, Y., Obata, Y., Takayama, K. Latent Structure Analysis of the Process Variables and Pharmaceutical Responses of an Orally Disintegrating Tablet, *Chem. Pharm. Bull.,* 60, 1419-1425 (2012).

59. Hirata, M., Takayama, K., Nagai, T. Formulation Optimization of Sustained-Release Tablet of Chlorpheniramine Maleate by Means of Extreme Vertices Design and Simultaneous Optimization Technique, *Chem. Pharm. Bull.,* 40, 741-746 (1992).

60. Procopio, A. T., Zavaliangos, A., Cunningham, J. C. Analysis of the diametrical compression test and the applicability to plastically deforming materials, *J. Mater. Sci.,* 38, 3629-3639 (2003).

61. Podczeck, F., Newton, J. M., Fromme, P. The bending strength of tablets with a breaking line—Comparison of the results of an elastic and a "brittle cracking" finite element model with experimental findings. *Int. J. Pharm.,* 495, 485-499 (2015).